Journal of Theoretical and Applied Information Technology
28th February 2023. Vol.101. No 4

ISSN: 1992-8645 www.jatit.org E-ISSN: 1817-3195

RESILIENT ARTIFICIAL FISH SWARM OPTIMIZATION-BASED ENHANCED CONVOLUTIONAL NEURAL NETWORK FOR AUTISM SPECTRUM DISORDER CLASSIFICATION

B. SURESH KUMAR[1], D. JAYARAJ[2]

[1]Assistant Professor, Department of Computer and Information Science, Annamalai University, India
[2]Assistant Professor, Department of Computer Science Engineering, Annamalai University, India
E-mail: [1]sureshaucis@gmail.com, [2]jayarajvnr@gmail.com

ABSTRACT

Autism Spectrum Disorder (ASD) is on the rise, making early diagnosis and intervention crucial for those living with the illness. The functional connectivity deficits in ASD have been employed with neuroimaging approaches to describe complicated biomarkers. ASD is still often diagnosed using a symptom checklist gleaned through in-person evaluations. Existing computer approaches sometimes produce inaccurate diagnostic categorization when applied to massive aggregated data sets. This paper proposes a novel bio-inspired optimization-based classification model combining convolution neural network and fish swarm optimization, namely Resilient Artificial Fish Swarm Optimization-based Enhanced Convolutional Neural Network ($RAFSO-ECNN$). $RAFSO-ECNN$is powered with three optimized behaviors derived from the natural characteristics of fishes. The performance of $ECNN$ Layers is strengthened with $RAFSO$. The performance of the $RAFSO-ECNN$ is evaluated with the Autism Brain Imaging Data Exchange II ($ABIDE-II$) dataset, a global multisite collection of functional and structural brain imaging data. The classification accuracy and the f-measure of $RAFSO-ECNN$ are much higher than those of the state-of-the-art classifiers.

Keywords: *Autism, Classification, Optimization, Convolutional Neural Network, Fish Swarm*

1. INTRODUCTION

Image classification is a crucial aspect of many problems that may be addressed using medical imaging. For example, image classification is frequently used to identify lesions and rule out potentially harmful normal tissues [1]. Tissues may be categorized to reveal object boundaries, which can be used in segmentation tasks. Classifying images that may be used to identify specific diseases or biomarkers is frequently the ultimate goal of medical imaging analysis. The classification of images is complicated by factors such as the high degree of intra-class variation and the lack of clarity across classes. It would be ideal if pictures in the same class looked the same while pictures in separate classes looked different [2]. These features would provide for efficient and simple image classification. Images belonging to the same class may share some similarities in appearance. However, this is usually not the case due to the diversity of visual patterns that make up each class and the inherent inter-subject variability. Low contrast between structures and tissues could make it hard to tell which images belong to which classes. Because of the prevalence of ambiguity in neuroimaging, image classification can be difficult [3].

Numerous medical image processing activities depend on locating anatomical landmarks and reference points. Clinical metrics for diagnosis and therapy planning can be computed once steps like image registration and segmentation algorithm setup have been completed. Manually identifying anatomical landmarks may seem difficult, but it is sometimes time-consuming and awkward [4]. When the exact localization of several landmarks is required, fast and accurate automated landmark localization methods may be extremely beneficial. Different ways to automatically find landmarks; some are made for specific uses or applications. These approaches may combine the segmentation of the landmarks' structures with local rule-based analysis. Multi-atlas image registration and ML are two technologies that can be used for more general

localization [5]. Multi-atlas image registration involves finding a match between the target image and several reference images that already have landmarks marked in them. After that, a popular vote is taken to determine where certain landmarks will be placed. Although such procedures are usually accurate and forgiving of anatomical and image capture differences, they can be time-consuming to put into practice. ML is faster and more accurate than previous approaches [6].

Commonplace ML techniques for medical image landmark localization often rely on classification or regression. Slices, patches, and voxels of an image can be analyzed using classification-based algorithms to identify the existence of a landmark. In classification, no grey area exists; a landmark is either absent or present [7]. As a result, the success of these techniques hinges on selecting an appropriate predefined threshold, which may vary depending on the data and the nature of the task at hand. Rather than relying on a discrete number as a cutoff, regression-based techniques produce a continuous score. Regression-based algorithms can determine how far or far away a landmark is by only looking at the image's slices, patches, or voxels [8].

1.1 Autism Spectrum Disorder

ASD indicates a neurodevelopmental disease with underlying cognitive traits and a high heritability rate; it often co-occurs with other illnesses. Researchers and practitioners have been interested in the traits, abilities, and difficulties of autistic people for at least 500 years [9]. Since its classification as a subtype under the wide diagnostic category of "pervasive developmental disorders," the word "autism" has been used in a variety of ways to represent both a more generalized appearance and a particular diagnosis (PDDs). Symptoms of autism range from mild to severe intellectual disability to difficulties with social communication and interaction, abnormal sensory processing, and repetitive behaviors [10]. Hyperactivity and attention problems, anxiety, depression, and seizures are quite frequent in people with autism and often co-occur with the core symptoms. A child is usually diagnosed with autism based on what the parents say about how the child has grown and acts around other people [11]. Children with autism often have trouble communicating, so early intervention is crucial. Parents and therapists may play a role in facilitating treatments for young children, while adolescents and young adults benefit from school-based procedures and approaches designed to foster autonomy [12]. Some signs and symptoms of autism and its comorbidities, such as irritability and anxiety, may be alleviated with pharmaceutical interventions. The treatment and management of autistic individuals and the condition's epidemiology and underlying mechanisms are highly significant. There are three main topics covered in this article: the underlying processes that cause autism, the variation among autistic people, and the lifelong effects of the disorder [13], [14].

It is often believed that the prevalence of autism is rising. However, this belief is grounded in speculation rather than evidence from community-based research and is supported only by statistics from administrative records. After researchers accounted for methodological differences across studies, they found no convincing evidence of a rise or fall in autism's frequency in the general population between 1990 and 2010. Prevalence rates in children and adults have not changed much over time, as proven by population-based and community-based case-finding surveys [15]. No strong data suggests that autism is less common among the elderly, which is another evidence against the hypothesis that autism's incidence is growing. Data indicates that individuals with autism are underdiagnosed even in high-income nations with robust autism public health strategies. In contrast, the number of children with autism who are administratively documented as having the disorder rises steadily [16]. This discovery underlines the need for collecting data on autism prevalence in situations where professionals may work to raise awareness. It is thought that 4% and 9% of people in mental health facilities have autism, which is much higher than in the general population [17].

In India, attitudes regarding disability need to be considered concerning autism. In many cultures, people with disabilities are looked down upon and treated with shame and disgrace because of the implication that their parents failed them in some way [18]. Unusual behaviors associated with autism have been linked to the development of myths regarding the disorder's cause. Historically, families concealed their odd children due to the social shame attached to them [19]. Seeing autistic children was a barrier to acceptance since they did not exist without seeing them. In doing so, it separated households, perpetuating the cycle of lack of education and belief in supernatural phenomena. The prejudice and lack of acceptance have

decreased in recent years. The media's function in raising consciousness is discussed further [20]. Over the last two decades, the autism campaign in India has made great strides. More people are diagnosed with autism at younger ages, more resources are available to meet the needs of people with autism, and the general public is more aware of the disorder [21]. However, a considerable amount of effort is still required. If people with autism are to be allowed to reach their full potential and live dignified lives in the future, parents, siblings, other family members, and professionals must continue to work together to advocate for rights that are frequently overlooked and vulnerable sectors [22].

1.2 Problem Statement

Even though ASD cannot be completely cured, early discovery of its signs may assist reduce the disease's impact. Due to the presence of other mental health conditions sharing similar symptoms, screening and analysis of ASD may be fairly difficult, leading in some instances to erroneous detection (i.e., misclassification). The long-term costs associated with a delayed diagnosis of ASD may be reduced if the disorder is identified and treated early, benefiting both patients and healthcare providers. Clinical procedures used in the past, such as the Autism-Diagnostic Observation-Schedule-Revised (ADOS-R) and Autism-Diagnostic Interview-Revised (ADIR), are laborious and time-consuming. The significant disadvantage of using clinical procedures in identifying ASD is the cost. Diagnosing ASD involves more cost. One of the most significant modern techniques is Deep learning (DL). Based on new approaches developed over the last decade that have become key instruments in healthcare, DL altered the diagnostic process to improve accuracy. Expense reduction is a primary motivation for utilizing DL in ASD diagnosis.

1.3 Objective

With the ABIDE II dataset containing fMRI scan images, the fundamental objective of this study is to propose a classifier, namely a Resilient Artificial Fish Swarm Optimization-based Enhanced Convolutional Neural Network that can accurately detect the existence of ASD.

1.4 Organization of the Paper

Section 1 discussed the digital image processing techniques, ASD, the problem statement, and the goal of the research. The state-of-the-art on how to classify ASD is reviewed in Section 2. The novel bio-inspired deep learning approach to ASD diagnosis is presented in Section 3. Section 4 provides a discussion about ABIDE II dataset. The performance criteria used to compare the proposed classifier against the state-of-the-art classifier are provided in Section 5. Section 6 presents the results and their subsequent discussion. The conclusion and potential improvements are described in Section 7.

2. LITERATURE REVIEW

"Behavior-based automated screening method to identify high-risk ASD" [23] is proposed for detecting infants aged 8-24 months. Multiple cues of the baby's response behavior are analyzed statistically, and an automated model is built. Also, an SVM classifier is employed to screen the performance level through experimental results. "Electrocardiograms, respiration, skin conductance and temperature" [24] are the physiological measurements used for reliable estimation of ASD. The positive and negative stimuli are evoked, and their intensity is tested. The accuracy is also measured, and its feasibility level is calculated. "Neurotypical Development" [25] is used for carrying out handwriting and speech tasks to measure the efficacy of ASD. Eigenvalues are derived, and children affected with ASD and TD are differentiated. Results were generated to assess the disease, and the progression of motor and speech interventions was validated. "Gaze-Sensitive" [26], along with peripheral augmentation, is carried out in the proposed study through different social situations to quantify task-based measurement and its performance. The proof of application structure for the VR-enabled platform is synchronized with gaze-based constraints, and results are generated. The task efficiency portrays its emotions using gaze-based biomarkers.

"Joint Attention" [27] is based on virtual reality to predict ASD in reality. The prompting level is increased, and results are generated based on the age factor of ASD and TD individuals. Also, the finger-pointing cue works better than other impairments for ASD-affected people and TD participants. "Robotic Agents" [28] are presented to detect the possessions of social stimuli through robotic agents for analyzing the attentional behavior of children affected with ASD. Participants with motion, visual and speech stimuli are considered for the study. The paired stimuli are found with positive correlations of positive values through the Pearson correlation function, and results are

executed. "Augmented Reality-based Tools" [29] are incorporated into the Google Cardboard with a head-mounted display in the present study. Analysis of the relationship among the facial expressions is carried out, and the toddlers are covered with cartoon faces. Results are generated, and the performance is increased in predicting psycho-pedagogical actions to guide the children with executive functionalities. **"**Thermal Imaging Modality" [30] is used to analyze the affective state and physiological signals along with temperature changes caused due to blood flow in blood vessels measured with the modality of autistic children. The experimental setup is structured, and the wavelet technique is deployed for detecting the patterns which modify due to different measures of interest. Results prove its efficiency with a better performance rate.

"ASC-Inclusion Platform" [31] combines multiple analytical tools, webcam, and onboard microphone functionalities. Training games, animations, video, audio clips and text-based formats are used to evaluate and detect different modalities. It also interprets verbal and non-verbal communication while making social interactions. "Virtual Reality" [32] based on facial expression is developed to track eye gaze by exploring the therapeutic prototype. A usage learning strategy is followed to detect the emotions and track the eye gaze where the inter and intragroup differences are exposed. The performance of the physiological features and the eye-tracking keys were recognized, and a comparison was performed. Results are generated, and the recognition rate is improved. The "Hilbert-Huang transform (HHT)" [33] technique is used to extract the features from a biomedical signal. For this, fMRI is used to explore clustering, and a Default Neural Network is used to detect the frequency bands. The three different cortexes, namely (i) cingulate, (ii) medial prefrontal, and (iii) anterior cingulate, are clustered together for predicting ASD using neuroimaging biomarkers. "VR-based interactive system" [34] is evolved in the study to demonstrate the viewing structures of ASD impairment. Gaze-sensitive technology and eye-tracking technique are integrated, facilitating engagement tasks. The real-time viewing structures are measured and evaluated using performance metrics with everyday social actions.

"Automated Motion Analysis" [35] is performed using body part movements, and the audio-visual understanding of speech is gathered for indexing. Also, individuals with autism and typically developing are segregated in which less complex actions are predicted. Experiments were carried out, and results were generated. The multisensory abilities are shaped, and their significance is enumerated. **"**Brain Network-Based Features**"** [36] are retrieved for diagnosis of neuro dysfunction of ASD in the proposed study. Through fMRI, two hundred sixty-four regions of packet structures are built, and the Laplacian matrix and network centralities are generated. Different features are developed, and the model is trained with the retrieved features. The classification accuracy is generated and is proving to be the highest accurate method of diagnosis. Successful applications of bio-inspired optimization have expanded into new fields like advanced networking [37]–[45], cyber security, medical image mining, share market prediction, etc.

"Genetic-Evolutionary Random Support Vector Machine (GERSVM)**"** [46] is proposed in which the cluster of SVMs randomly picks the samples and the features. The genetic evolution is mutated, and classification accuracy is validated for stability. Resting-state fMRI is used to find abnormal brain regions and prove to assist in the diagnosis of ASD. Recursive Cluster Elimination-based Support Vector Machine (RCE-SVM) is one among the machine learning-based classification approach used by "Functional Connectivity Complex Network Measures (FC-CNM)" [47] to evaluate the prediction efficiency of conventional connectivity and complex network measures that are obtained from ABIDE dataset. The prediction performance of three separate feature sets was investigated using RCE-SVM: (1) Functional Connectivity, (2) Complex Network Measures, and (3) a mixture of both 1 and 2. FC-CNM is divided into three stages: Clustering features, calculating feature relevance for cluster classification and removing clusters with low scores using RCE.

3. RESILIENT ARTIFICIAL FISH SWARM OPTIMIZATION-BASED ENHANCED CONVOLUTIONAL NEURAL NETWORK

3.1 Enhanced Convolution Neural Network

The cat's cerebral cortex inspires the network model Enhanced Convolutional Neural Network ($ECNN$), which is sensitive to local changes and selective in how it processes information in the dataset. This type of bio-neural network has a structure that greatly simplifies the model and the number of learning parameters. $ECNN$significantly uses three different layers to extract characteristics from input images. The multi-layer network model

is used in supervised learning for classification and ends in the result of providing the outputs (i.e., attributes).

3.1.1 Convolution Layer (CL)

In CL, to extract, filter, and improve features of images, it is necessary to load images into the network's input layer and convolve it using the convolution kernel. Finally, the activation function is used to get the layer's extracted features, which are denoted by the index q_w^z. Eqn.(1) is used to represent the same.

$$q_w^z = g\left(\sum_{s\omega M_w}\left(a_{s,w}^z \times q_s^{z-1}\right) + \sum\left(v_w^z\right)\right) \quad (1)$$

In Eqn.(1), $g(.)$ is the activation function for the hidden layer, z expresses the number of layers, $a_{s,w}$ is the convolution kernel, $*$ is the $2Y$ permutation operation, v_w bias, M_w expresses the set of input features that are selected, and q_w^z expresses the wth extracted features of the zth layer.

In CL, this research evaluates the nonlinear-based activation function i.e., sigmoid in contrast to the regular unit of correction RLU (i.e., Rectified Linear Unit), which is defined as Eqn.(2) and Eqn.(3):

$$sigmoid: g(p) = \frac{1}{1+h^{-p}} \quad (2)$$

$$RLU: g(p) = \begin{cases} 0, p < 0 \\ p, p > 0 \end{cases} \quad (3)$$

where in p is the excitation function's argument, denoted by the numbers within the brackets in Eqn.(1).

3.1.2 Down Sampling Layer (DSL)

In CL, the output features are down-sampled to prevent an unreasonably high computation cost caused by the excessive dimension of the large feature. After the bias operation, the down-sampled output characteristic is obtained by averaging the $t \times t$ image pools using a unique sliding window. Pixels present in the image pool can be down-sampled either by the average pooling method (APM) or the Maximum Pooling Method (MPM), as illustrated in Eqn.(4).

$$q_w^z = \prod j(down(q_s^{z-1}).n_w^z + v_w^z) \quad (4)$$

In Eqn.(4), $down(.)$ indicates sub-sampling function, n_w^z is the DSL's weight coefficient, and v_w^z is the layer's bias. This research work utilizes MPM to reduce the number of features while maintaining valid image information.

3.1.3 Fully Connected Layer (FCL)

The input of FCL is the one-dimensional eigenvector created by enhancing all the neurons present in the feature of one-dimensional images. In FCL, every neuron is linked to every other in higher-level capabilities. This assists in getting the output via applying the activation function mapping and the summation sum. Eqn.(5) expresses the same.

$$K_{sw}^z = \sum sigm((n^z * o)_{sw} + v_z) \quad (5)$$

while $sigm(.)$ is the FCL's activation function, n^z represents the weight coefficient, o is its feature input, v_z indicates the offset of FCL, s and w are its respective index numbers in two-dimensional coordinates.

3.2 Resilient Artificial Fish Swarm Optimization (RAFSO)

Non-dominated optimum solutions are evacuated via the proposed optimization strategy, i.e., $RAFSO$. It employs the multi-objective idea to solve the ASD classification issue. To illustrate potential answers to the poor classification accuracy, it employs three different fish behaviors, namely, (i) Preying ($Pryg$), (ii) Swarming ($Swrg$) and (iii) Following ($Flwg$). $RAFSO$ gives importance to starting population of fish (i.e., the count), each of which represents a solution to (i) ASD classification issue and (ii) repository of all non-dominated ASD individuals. The behavior of each fish is determined once the population has been created.

3.2.1 Population Initialization

$RAFSO$ aims to converge rapidly to the optimal alignment while avoiding convergence simultaneously. $RAFSO$ offers a smart initialization strategy that combines the two different approaches. Firstly, to ensure all sequences are of equal length, $RAFSO$ randomly insert space between them. Secondly, a progressive alignment strategy is applied to identify the dependency on

the direction of the space offsets (i.e., either to the right or left).

In $RAFSO$, 65% of the initial population is generated in a general optimization manner, while the other 35% is created randomly. The first population split ensures a balance between exploration (i.e., discovery) and exploitation. $RAFSO$divides the original population in half to balance the two main goals, i.e., exploitation ($expli$) and exploration ($explr$). $RAFSO$initiating point falls between $expli$ and $explr$.

3.2.2 Objective Function

To determine the better classification, $RAFSO$ looks for the set of Pareto improvements that maximize the weights and similarities. When figuring out how much each residue pair should cost in the two-goal functions, $RAFSO$ turn to the two-substitution matrix. Eqn.(6) provides the approach of measuring the weights in $RAFSO$.

$$WPS = \sum_{s=1}^{a-1} \sum_{w=s+1}^{a} \left(n_s \times n_w \times score(E_s * E_w)\right) \quad (6)$$

$$Score(E_s, E_w) = \begin{cases} d \ if \ E_s = E_w \\ v \ if \ E_s \neq E_w \ and \ E_s \neq \text{`_`} \ \text{or} \ E_w = \text{`_`} \\ u \ if \ E_s \neq E_w \ and \ E_s = \text{`_`} \ \text{and} \ E_s \neq \text{`_`} \end{cases} \quad (7)$$

where$a$ is the total number of sequences, and d, v, and u are the corresponding values for the number of matches, mismatches, and spaces. Scores of d and v are produced using the scoring method, and a score of u is derived using a specific penalty model. The phylogenetic tree strategies are applied to yield sequence weights of E_s and E_w for $s$and w, respectively.

- In bio-inspiration, the cost of making space is substantially higher than the cost of increasing it. This may be achieved by increasing the cost of the space opening in proportion to its size. The cost of space is usually denoted as sop (space opening penalty). Extending spaces is done with the help of sep (space extending penalty). If $RAFSO$ take the affine function, i.e., $space(Z) = sop + (Z-1) * sep$, then the calculation of cost for the space with length Z.
- To create a matrix for conventional replacement, sop values of around -1 and sep values of around -10 are often employed as the default. These numbers are always generated randomly. However, they should generally stay around a $sop/sep$of 1.

3.2.3 Swarming

The fish will gather together at different locations via a relocation process to secure the colony's survival and protect itself from classification errors. Here, $RAFSO$ uses the consensus sequence approach to identify the centre ($Cent_u$) of the school (i.e., a group of fish). Suppose that $Cent_s$ is the present position of the fish, then $Cent_u$ is the Central Fish, and $Cent$ is the number of other fishes in the immediate area (Distance $(Cent_s, Cent_u) < (Visual_s)$, and t is the population size. Unless $\left((Cent_u \prec Cent_s) \text{ and } \left(\frac{tg}{t} < \theta\right)\right)$, which implies that the companion centre has more food (i.e., $Cent_u$ dominates$Cent_s$) and is not particularly crowded, the $Cent$ moves one step toward the companion centre by doing a crossover procedure, either once or more than once among $Cent_s$ and $Cent_u$. Eqn.(8) expresses the swarming behavior of $RAFSO$.

$$DG_s^{(f+1)} = Crossover(DG_s, DG_u) \quad (8)$$

If not, the $Cent\_Prey$ action is taken. At a vast field, the swarm size is constrained by the crowding effect, and the $Cent$ will get clustered in the optimal location. Thus, the $Cent$ always find their best cum superior location.

3.2.4 Following

When one or more of the fish in a school finds food while moving from one location to another, the other artificial fish in the school will rapidly follow in its wake. Assume that $Cent$ is the current $Cent$ and that $Cent_v$ is the optimum fish among $Cent_s$, which verifies $Cent_v / (Cent_v \prec Cent_w) \forall (Distance\ (Cent_s, Cent_w) < Visual)$. Unless $\left((Cent_v \prec Cent_s) \ and \ \left(\frac{tg}{t} < \theta\right)\right)$, it implies that the companion $Cent_v$ has a higher food concentration where $Cent_v$ dominates $Cent_s$. When the school is not too crowded, then the $Cent_s$ moves forward one step to the companion $Cent_s$ via crossover operation $Cent_v$. Eqn.(9) exhibits the $Following$ behavior.

$$Cent_s^{(f+1)} = Crossover(Cent_s, Cent_v) \quad (9)$$

If none of them was satisfied, then $Preying$ behavior is followed.

Journal of Theoretical and Applied Information Technology
28th February 2023. Vol.101. No 4

ISSN: 1992-8645 www.jatit.org E-ISSN: 1817-3195

3.2.5 Preying

Preying is a natural cum instinctive response that ensures the species' survival. The fish use their eyesight to detect the density of food particles in the water, which they subsequently use to guide their direction of travel. Let $Cent_s$ be the $Cent$ currently, and then pick an $Cent_w$ at random by mutating its visual distance $(Distance(Cent_s, Cent_w) < Visual)$.

$$Cent_w = \sum Mutation(Cent_s) \quad (10)$$

To advance in this way, if ($Cent_w$dominates $Cent_s$) then $(Cent_w \prec Cent_s)$ occurs; the $Cent_s$ then crosses over to its best neighbor either once or more than once.

$$Cent_s^{(f+1)} = Crossover(Cent_s, Cent_w) \quad (11)$$

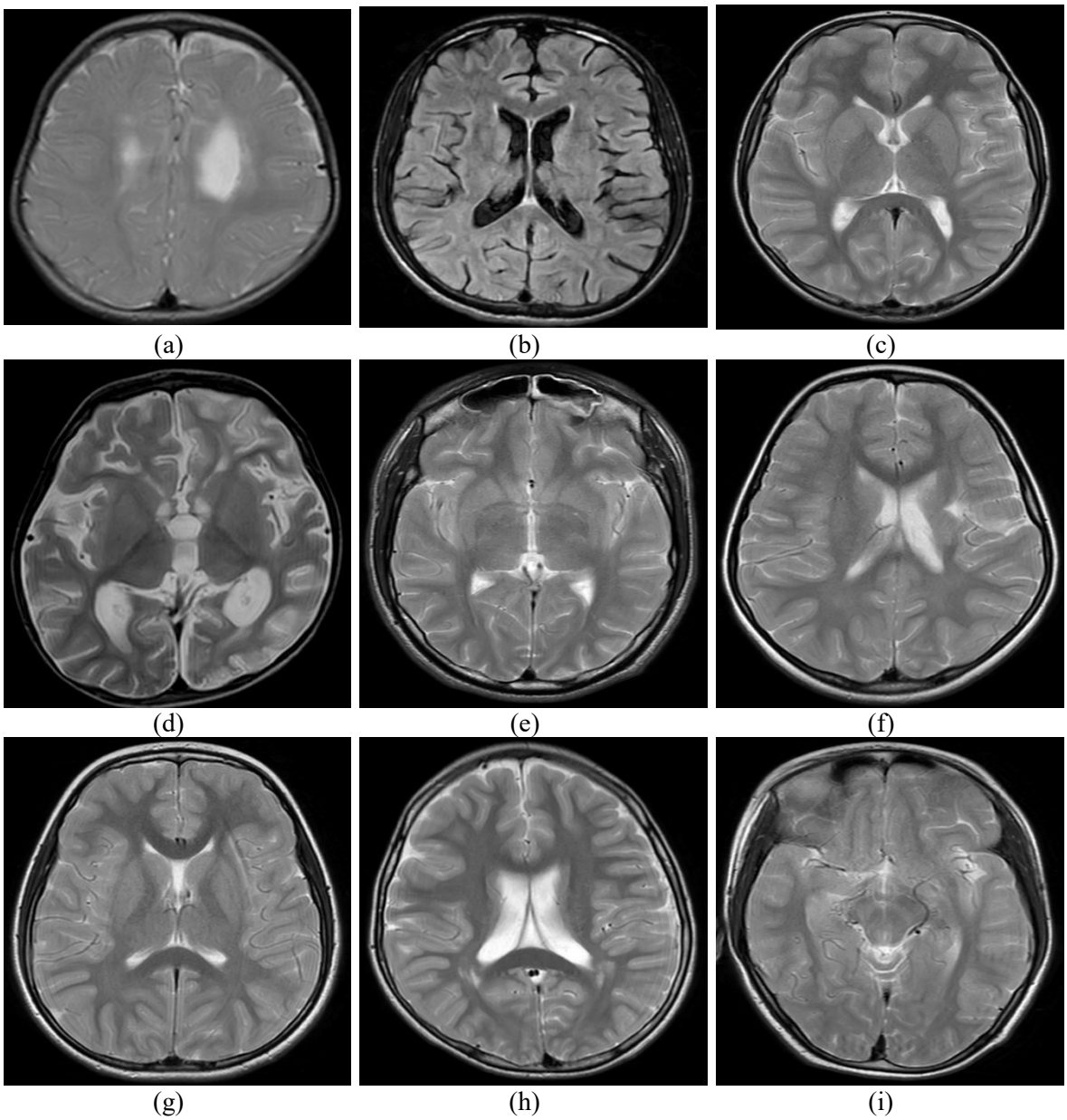

Fig 1 Autistic Fmri Brain Images

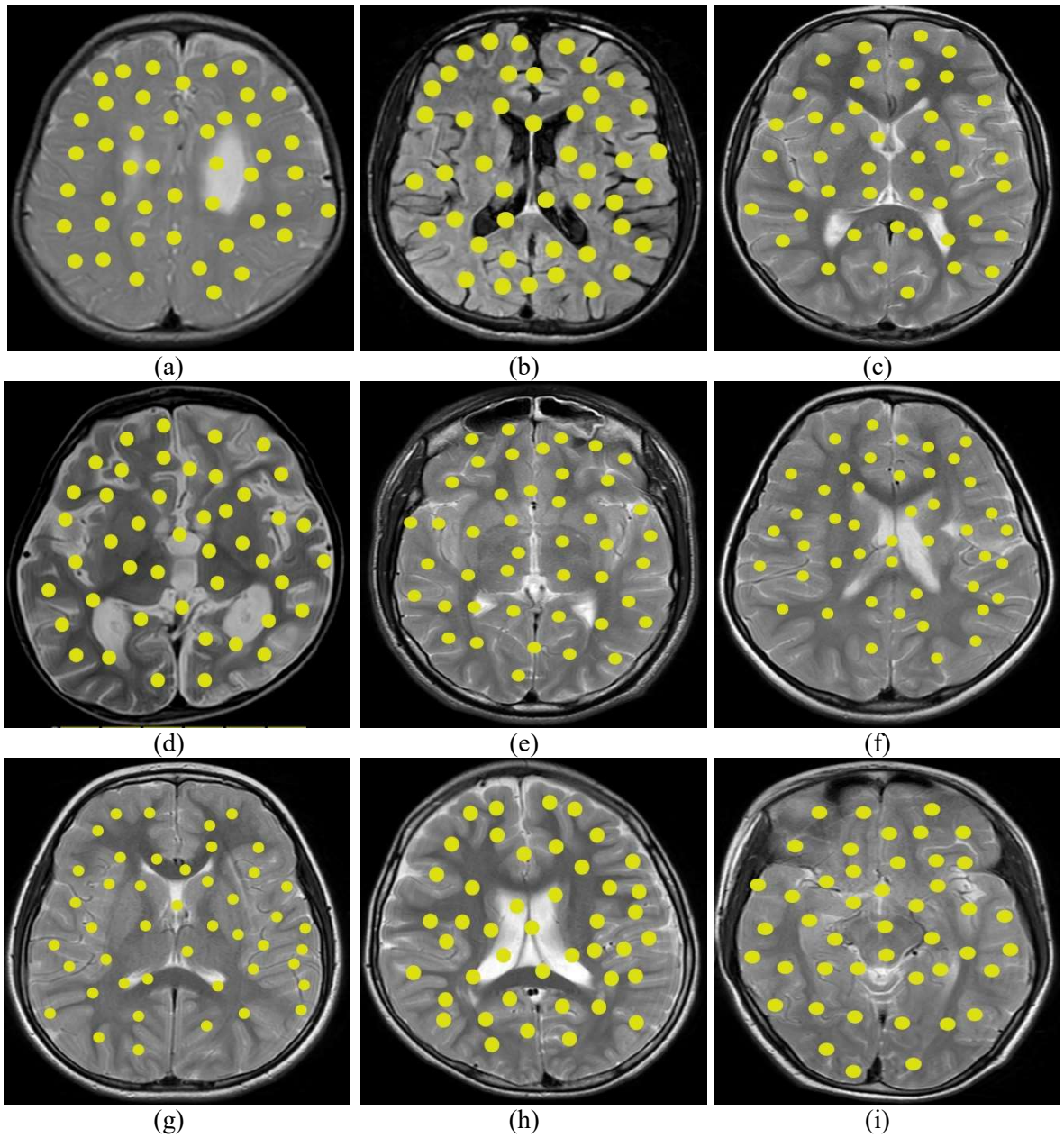

Fig 2 Autistic Brain Regions Detected By $RAFSO - ECNN$

If not, pick another $Cent_w$ at random and evaluate whether it meets the forwarding condition. After trying the threshold number of times with zero success, it randomly switches to a neighboring option.

3.3 Fusion of ECNN and RAFSO

$FCLofECNN$ plays a significant role in classification, and it seems to have less potential while enhancing the performance of FCL will lead to better classification accuracy. This research work applies the $RAFSO$ in FCL to enhance the performance of the neurons leading to a better classificationof ASD.

4. ABOUT THE DATASET

The utility and efficacy of ABIDE I's setup for pooling MRI data from many sites were demonstrated. However, the complexity of the connectome, the wide heterogeneity of ASD, and the first results of the ABIDE I data analysis all indicate the need for much larger and better-characterized samples. With support from the National Institute of Mental Health (R21MH107045), ABIDE II was established to

further the field of connectome discovery in autism spectrum disorder. Since the project's inception, the phenotypic characterization of ABIDE II datasets, particularly those evaluating core ASD and associated symptoms, has grown by over a thousand. Furthermore, two sets of data include longitudinal samples from 38 people collected across two time periods (i.e., the interval of one to four years). ABIDE II now has 19 locations participating, encompassing 10 charter institutions and 7 new members, who have submitted 1114 datasets comprising data on 521 persons with ASD and 593 controls (range of age falls between 5 and 64 years). This data was made available free to the public in June 2016. As required by HIPAA and the criteria employed by the 1000 Functional Connectomes Project/INDI, no personally identifiable information is included in any of the datasets. Figure 1 provides the sample images. The fMRI images hold the pixel values of 256×256.

5. PERFORMANCE METRICS

This research compares $RAFSO-ECNN$ against $GERSVM$ and $FC-CNM$ using the standard sum benchmark performance criteria listed below.

- Classification Accuracy ($Cl-Acc$): The effectiveness of a classification model may be summarized by its classification accuracy, which is calculated by dividing the proportion of right predictions by the total number of predictions.
- F-Measure ($F-Msr$): It is a method for integrating classifier performance metrics that emphasizes a harmonic mean of recall and precision.
- Fowlkes-Mallows Index (FMI): It is the geometric mean of recall and precision results.
- Matthews Correlation Coefficient (MCC): It is a criterion for evaluating the accuracy of the actual and expected results.

The above-mentioned each performance metric utilizes (1) True-Positive ($Tr-Pos$), (2) False-Positive ($Fl-Pos$), (3) True-Negative ($Tr-Neg$), and (4) False-Negative ($Fl-Neg$), for the calculation.

6. RESULTS AND DISCUSSION

6.1 ASD detection by RAFSO-ECNN

Figure 2 highlights the autistic brain regions that are identified by the proposed classifier $RAFSO-ECNN$ while evaluating in MATLAB 2021b.

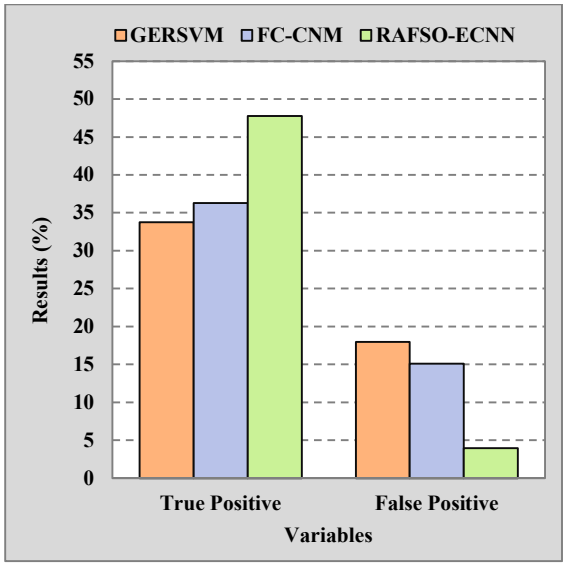

Fig 3 $Tr-Pos$ and $Fl-Pos$ Analysis

6.2 Positivity Analysis

Evaluation of positive results (i.e., $Tr-Pos$and $Fl-Pos$) are carried out in Figure 3. The $X-axis$ displays $Tr-Pos$ and $Fl-Pos$ as independent variables. The $Y-axis$ displays percentages of $Tr-Pos$ and $Fl-Pos$ results. As shown in Figure 3, $RAFSO-ECNN$ outperforms both $GERSVM$and $FC-CNM$. The optimized way of down-sampling leads $RAFSO-ECNN$ to gain increased performance in terms of $Tr-Pos$and $Fl-Pos$. Due to having no optimization, $GERSVM$ and $FC-CNM$ achieves low $Tr-Pos$and $Fl-Pos$. Table 1 holds the values of $Tr-Pos$ and $Fl-Pos$ results that were established during the assessment of classifiers.

Table 1 $Tr-Pos$ and $Fl-Pos$ result values

Algorithms	$Tr-Pos$	$Fl-Pos$
GERSVM	33.752	17.953
FC-CNM	36.266	15.081
RAFSO-ECNN	47.756	3.950

Journal of Theoretical and Applied Information Technology
28th February 2023. Vol.101. No 4

ISSN: 1992-8645 www.jatit.org E-ISSN: 1817-3195

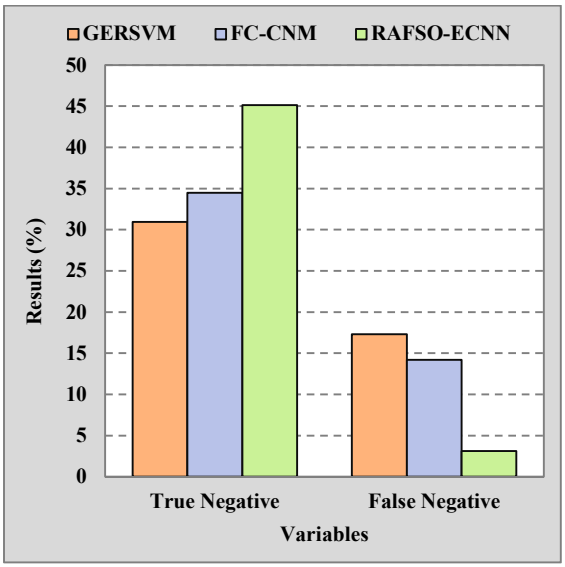

Fig 4 $Tr-Neg$ and $Fl-Neg$ Analysis

Table 2 $Tr-Neg$ and $Fl-Neg$ result values

Algorithms	$Tr-Neg$	$Fl-Neg$
GERSVM	30.969	17.325
FC-CNM	34.470	14.183
RAFSO-ECNN	45.153	3.142

6.3 Negativity Analysis

Figure 4 examines the classifier assessment negative results (i.e., $Tr-Neg$and $Fl-Neg$). $Tr-Neg$and$Fl-Neg$ are the variables that are plotted along the $X-axis$. The $Y-axis$ displays the percentage of results obtained for $Tr-Neg$and $Fl-Neg$. Compared to $GERSVM$and $FC-CNM$, $RAFSO-ECNN$ performs better, as seen in Figure 4. The swarming strategy used in $RAFSO-ECNN$ assists in achieving the better result in $Tr-Neg$and $Fl-Neg$, i.e., increased $Tr-Neg$ and decreased $Fl-Neg$. $GERSVM$and$FC-CNM$ prefer first-come-first-served based classification without any optimization, which results in negativity analysis. Table 2 illustrates the obtained result values of $Tr-Neg$ and $Fl-Neg$ during the evaluation.

6.4 $Cl-Acc$ and $F-Msr$ Analysis

Results from the proposed and existing classifiers are compared and contrasted in Figure 5 for $Cl-Acc$and $F-Msr$. On the $X-axis$, $Cl-Acc$ and $F-Msr$ are plotted, and on the $Y-axis$, the percentage of attained outcomes are plotted. Based on the results displayed in Figure 5, it is clear that $RAFSO-ECNN$ performs better than both $GERSVM$and $FC-CNM$. Preying behavior of $RAFSO-ECNN$ leads a way to detect ASD and $non-ASD$ more accurately that results in increased $Cl-Acc$. $F-Msr$demonstrates how far the $Cl-Acc$ is true. The results of the classifier evaluation are listed in Table 3, including $Cl-Acc$ and $F-Msr$ values.

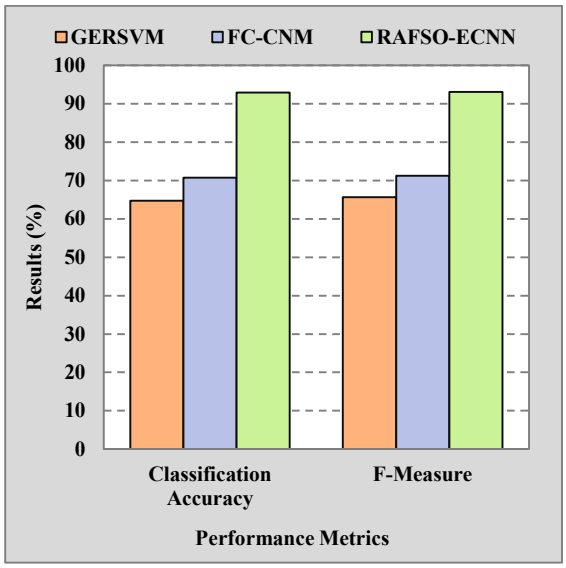

Fig 5 $Cl-Acc$ and $F-Msr$ Analysis

Table 3 $Cl-Acc$ and $F-Msr$ Result Values

Algorithms	$Cl-Acc$	$F-Msr$
GERSVM	64.722	65.677
FC-CNM	70.736	71.252
RAFSO-ECNN	92.908	93.088

6.5 FMIandMCC Analysis

In Figure 6, it is possible to see a contrast between the proposed and existing classifiers for FMI and MCC results. The $X-axis$ displays FMI and MCC metrics, while the $Y-axis$ displays the attained results. Figure 6 shows that $RAFSO-ECNN$ outperforms $GERSVM$and $FC-CNM$. The three different behaviors of $RAFSO-ECNN$ play a significant role in achieving better $FMI$and MCC. All three behaviors focus only on a single target of detecting ASD and $non-ASD$ more accurately. $GERSVM$and$FC-CNM$ do not have different processes or functions to ASD and $non-ASD$ detection leading to poor FMI and MCC. The outcomes of the tests conducted on the proposed and existing classifiers for the FMI andMCC metrics are shown in Table 4.

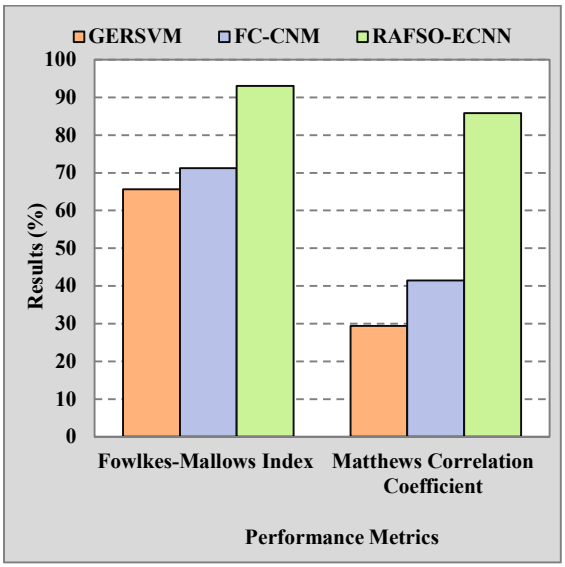

Fig 6FMI and MCC Analysis

Table 4 FMI and MCC Result Values

Algorithms	*FMI*	*MCC*
GERSVM	65.678	29.394
FC-CNM	71.255	41.465
RAFSO-ECNN	93.091	85.819

7. CONCLUSION

Autism spectrum disorders (ASD) encompass a group of neurodevelopmental diseases typically seen in young children, such as autism and Asperger's syndrome. To properly diagnose ASD using rs-fMRI data, Resilient Artificial Fish Swarm Optimization-Based Enhanced Convolutional Neural Network ($RAFSO-ECNN$) is introduced in this paper, which is a unique bio-inspired optimization-based classification algorithm inherited from the natural behavior of fishes. The performance of $ECNN$ are enhanced using $RAFSO$. Our model outperformed other state-of-the-art approaches with the greatest classification accuracy (92.908%). In-depth experiments proved beyond a reasonable doubt the consistent performance. This research work is a potential resource for using rs-fMRI data to identify individuals with ASD. We hypothesize that the suggested model, which combines bio-inspired optimization approaches with various neural network models, may shed light on the computer-assisted diagnosis of complicated psychiatric diseases.

REFERENCES:

[1]. X. Feng, B. Gong, C. Tang, and T. Zhao, "Study on the non-linear deformation and failure characteristics of EPS concrete based on CT-scanned structure modelling and cloud computing," *Eng. Fract. Mech.*, vol. 261, p. 108214, 2022, doi: https://doi.org/10.1016/j.engfracmech.2021.108214.

[2]. A. De, T. Vo, and M. Wright, "Value-offset bifiltrations for digital images," *Comput. Geom.*, vol. 109, p. 101939, 2023, doi: https://doi.org/10.1016/j.comgeo.2022.101939.

[3]. G. Deng *et al.*, "Digital image colorimetry in combination with chemometrics for the detection of carbaryl based on the peroxidase-like activity of nanoporphyrins and the etching process of gold nanoparticles," *Food Chem.*, vol. 394, p. 133495, 2022, doi: https://doi.org/10.1016/j.foodchem.2022.133495.

[4]. M. Hinderdael, J. Ertveldt, Z. Jardon, L. Pyl, and P. Guillaume, "Residual stress characterization during laser-based Directed Energy Deposition using in-situ digital image correlation based on specular light reflection on as-built surfaces of thin walls," *Procedia CIRP*, vol. 111, pp. 313–316, 2022, doi: https://doi.org/10.1016/j.procir.2022.08.029.

[5]. A. Kumar, K. Srinivasan, W.-H. Cheng, and A. Y. Zomaya, "Hybrid context enriched deep learning model for fine-grained sentiment analysis in textual and visual semiotic modality social data," *Inf. Process. Manag.*, vol. 57, no. 1, p. 102141, 2020, doi: https://doi.org/10.1016/j.ipm.2019.102141.

[6]. V. Yaneva, L. A. Ha, S. Eraslan, Y. Yesilada, and R. Mitkov, "Detecting High-Functioning Autism in Adults Using Eye Tracking and Machine Learning," *IEEE Trans. Neural Syst. Rehabil. Eng.*, vol. 28, no. 6, pp. 1254–1261, 2020, doi: 10.1109/TNSRE.2020.2991675.

[7]. B. Ferreira, J. Rodrigues, J. Leitão, and H. Domingos, "Practical Privacy-Preserving Content-Based Retrieval in Cloud Image Repositories," *IEEE Trans. Cloud Comput.*, vol. 7, no. 3, pp. 784–798, 2019, doi: 10.1109/TCC.2017.2669999.

[8]. X. Zhu, Z. Cheng, S. Wang, X. Chen, and G. Lu, "Coronary angiography image

segmentation based on PSPNet," *Comput. Methods Programs Biomed.*, vol. 200, p. 105897, 2021, doi: https://doi.org/10.1016/j.cmpb.2020.105897.

[9]. S. K. S. Raja and V. Balaji, "Sensor based learning device for children with autism," *Mater. Today Proc.*, vol. 50, pp. 307–311, 2022, doi: https://doi.org/10.1016/j.matpr.2021.07.380.

[10]. G. Nie *et al.*, "An Immersive Computer-Mediated Caregiver-Child Interaction System for Young Children With Autism Spectrum Disorder," *IEEE Trans. Neural Syst. Rehabil. Eng.*, vol. 29, pp. 884–893, 2021, doi: 10.1109/TNSRE.2021.3077480.

[11]. E. Stevens, D. R. Dixon, M. N. Novack, D. Granpeesheh, T. Smith, and E. Linstead, "Identification and analysis of behavioral phenotypes in autism spectrum disorder via unsupervised machine learning," *Int. J. Med. Inform.*, vol. 129, pp. 29–36, 2019, doi: https://doi.org/10.1016/j.ijmedinf.2019.05.006.

[12]. A. S. Heinsfeld, A. R. Franco, R. C. Craddock, A. Buchweitz, and F. Meneguzzi, "Identification of autism spectrum disorder using deep learning and the ABIDE dataset," *NeuroImage Clin.*, vol. 17, pp. 16–23, 2018, doi: https://doi.org/10.1016/j.nicl.2017.08.017.

[13]. S. Gyawali, B.N. Patra, "Autism spectrum disorder: Trends in research exploring etiopathogenesis". Psychiatry Clin. Neurosci., vol. 73, pp. 466-475. doi: https://doi.org/10.1111/pcn.12860

[14]. M. Hirokawa, A. Funahashi, Y. Itoh, and K. Suzuki, "Adaptive Behavior Acquisition of a Robot Based on Affective Feedback and Improvised Teleoperation," *IEEE Trans. Cogn. Dev. Syst.*, vol. 11, no. 3, pp. 405–413, 2019, doi: 10.1109/TCDS.2018.2846778.

[15]. J. Wang *et al.*, "Automated interpretation of congenital heart disease from multi-view echocardiograms," *Med. Image Anal.*, vol. 69, p. 101942, 2021, doi: https://doi.org/10.1016/j.media.2020.101942.

[16]. P. R. K. Babu and U. Lahiri, "Multiplayer Interaction Platform With Gaze Tracking for Individuals With Autism," *IEEE Trans. Neural Syst. Rehabil. Eng.*, vol. 28, no. 11, pp. 2443–2450, 2020, doi: 10.1109/TNSRE.2020.3026655.

[17]. M. Gök, "A novel machine learning model to predict autism spectrum disorders risk gene," *Neural Comput. Appl.*, vol. 31, no. 10, pp. 6711–6717, Oct. 2019, doi: 10.1007/s00521-018-3502-5.

[18]. J. M. Vicente-Samper, E. Ávila-Navarro, and J. M. Sabater-Navarro, "Data Acquisition Devices Towards a System for Monitoring Sensory Processing Disorders," *IEEE Access*, vol. 8, pp. 183596–183605, 2020, doi: 10.1109/ACCESS.2020.3029692.

[19]. J. Li *et al.*, "Appearance-Based Gaze Estimation for ASD Diagnosis," *IEEE Trans. Cybern.*, vol. 52, no. 7, pp. 6504–6517, 2022, doi: 10.1109/TCYB.2022.3165063.

[20]. L. Santos, A. Geminiani, P. Schydlo, I. Olivieri, J. Santos-Victor, and A. Pedrocchi, "Design of a Robotic Coach for Motor, Social and Cognitive Skills Training Toward Applications With ASD Children," *IEEE Trans. Neural Syst. Rehabil. Eng.*, vol. 29, pp. 1223–1232, 2021, doi: 10.1109/TNSRE.2021.3091320.

[21]. T. Vargason, E. Roth, G. Grivas, J. Ferina, R. E. Frye, and J. Hahn, "Classification of autism spectrum disorder from blood metabolites: Robustness to the presence of co-occurring conditions," *Res. Autism Spectr. Disord.*, vol. 77, p. 101644, 2020, doi: https://doi.org/10.1016/j.rasd.2020.101644.

[22]. L. Q. Uddin, "Brain Mechanisms Supporting Flexible Cognition and Behavior in Adolescents With Autism Spectrum Disorder," *Biol. Psychiatry*, vol. 89, no. 2, pp. 172–183, 2021, doi: https://doi.org/10.1016/j.biopsych.2020.05.010.

[23]. C. Tang *et al.*, "Automatic Identification of High-Risk Autism Spectrum Disorder: A Feasibility Study Using Video and Audio Data Under the Still-Face Paradigm," *IEEE Trans. Neural Syst. Rehabil. Eng.*, vol. 28, no. 11, pp. 2401–2410, 2020, doi: 10.1109/TNSRE.2020.3027756.

[24]. S. Sarabadani, L. C. Schudlo, A. A. Samadani, and A. Kushski, "Physiological Detection of Affective States in Children with Autism Spectrum Disorder," *IEEE Trans. Affect. Comput.*, vol. 11, no. 4, pp. 588–600, 2020, doi: 10.1109/TAFFC.2018.2820049.

[25]. T. Talkar *et al.*, "Assessment of Speech and Fine Motor Coordination in Children WithAutism Spectrum Disorder," *IEEE Access*, vol. 8, pp. 127535–127545, 2020, doi: 10.1109/ACCESS.2020.3007348.

[26]. P. R. K. Babu, P. Oza, and U. Lahiri, "Gaze-Sensitive Virtual Reality Based Social Communication Platform for Individuals with Autism," *IEEE Trans. Affect. Comput.*, vol. 9, no. 4, pp. 450–462, 2018, doi: 10.1109/TAFFC.2016.2641422.

[27]. V. Jyoti and U. Lahiri, "Virtual Reality Based Joint Attention Task Platform for Children With Autism," *IEEE Trans. Learn. Technol.*, vol. 13, no. 1, pp. 198–210, 2020, doi: 10.1109/TLT.2019.2912371.

[28]. F. Mehmood *et al.*, "Attentional Behavior of Children With ASD in Response to Robotic Agents," *IEEE Access*, vol. 9, pp. 31946–31955, 2021, doi: 10.1109/ACCESS.2021.3056211.

[29]. K. P. Soares, A. M. F. Burlamaqui, L. M. G. Goncalves, V. F. da Costa, M. E. Cunha, and A. A. R. S. da S. Burlamaqui, "Preliminary Studies With Augmented Reality Tool To Help In Psycho-pedagogical Tasks With Children Belonging To Autism Spectrum Disorder," *IEEE Lat. Am. Trans.*, vol. 15, no. 10, pp. 2017–2023, 2017, doi: 10.1109/TLA.2017.8071250.

[30]. N. Rusli, S. N. Sidek, H. M. Yusof, N. I. Ishak, M. Khalid, and A. A. A. Dzulkarnain, "Implementation of Wavelet Analysis on Thermal Images for Affective States Recognition of Children With Autism Spectrum Disorder," *IEEE Access*, vol. 8, pp. 120818–120834, 2020, doi: 10.1109/ACCESS.2020.3006004.

[31]. E. Marchi *et al.*, "The ASC-Inclusion Perceptual Serious Gaming Platform for Autistic Children," *IEEE Trans. Games*, vol. 11, no. 4, pp. 328–339, 2019, doi: 10.1109/TG.2018.2864640.

[32]. [32] E. Bekele, Z. Zheng, A. Swanson, J. Crittendon, Z. Warren, and N. Sarkar, "Understanding How Adolescents with Autism Respond to Facial Expressions in Virtual Reality Environments," *IEEE Trans. Vis. Comput. Graph.*, vol. 19, no. 4, pp. 711–720, 2013, doi: 10.1109/TVCG.2013.42.

[33]. H. Zhang, R. Li, X. Wen, Q. Li, and X. Wu, "Altered Time-Frequency Feature in Default Mode Network of Autism Based on Improved Hilbert-Huang Transform," *IEEE J. Biomed. Heal. Informatics*, vol. 25, no. 2, pp. 485–492, 2021, doi: 10.1109/JBHI.2020.2993109.

[34]. U. Lahiri, E. Bekele, E. Dohrmann, Z. Warren, and N. Sarkar, "Design of a Virtual Reality Based Adaptive Response Technology for Children With Autism," *IEEE Trans. Neural Syst. Rehabil. Eng.*, vol. 21, no. 1, pp. 55–64, 2013, doi: 10.1109/TNSRE.2012.2218618.

[35]. J.-P. Noel, M. A. De Niear, N. S. Lazzara, and M. T. Wallace, "Uncoupling Between Multisensory Temporal Function and Nonverbal Turn-Taking in Autism Spectrum Disorder," *IEEE Trans. Cogn. Dev. Syst.*, vol. 10, no. 4, pp. 973–982, 2018, doi: 10.1109/TCDS.2017.2778141.

[36]. S. Mostafa, L. Tang, and F. Wu, "Diagnosis of Autism Spectrum Disorder Based on Eigenvalues of Brain Networks," *IEEE Access*, vol. 7, pp. 128474–128486, 2019, doi: 10.1109/ACCESS.2019.2940198.

[37]. J. Ramkumar, "Bee inspired secured protocol for routing in cognitive radio ad hoc networks," *Indian J. Sci. Technol.*, vol. 13, no. 30, pp. 2159–2169, 2020, doi: 10.17485/ijst/v13i30.1152.

[38]. J. Ramkumar and R. Vadivel, "Improved frog leap inspired protocol (IFLIP) – for routing in cognitive radio ad hoc networks (CRAHN)," *World J. Eng.*, vol. 15, no. 2, pp. 306–311, 2018, doi: 10.1108/WJE-08-2017-0260.

[39]. J. Ramkumar and R. Vadivel, "Multi-Adaptive Routing Protocol for Internet of Things based Ad-hoc Networks," *Wirel. Pers. Commun.*, vol. 120, no. 2, pp. 887–909, Apr. 2021, doi: 10.1007/s11277-021-08495-z.

[40]. R. Jaganathan and R. Vadivel, "Intelligent Fish Swarm Inspired Protocol (IFSIP) for Dynamic Ideal Routing in Cognitive Radio Ad-Hoc Networks," *Int. J. Comput. Digit. Syst.*, vol. 10, no. 1, pp. 1063–1074, 2021, doi: 10.12785/ijcds/100196.

[41]. R. Jaganathan and V. Ramasamy, "Performance modeling of bio-inspired routing protocols in Cognitive Radio Ad Hoc Network to reduce end-to-end delay," *Int. J. Intell. Eng. Syst.*, vol. 12, no. 1, pp. 221–231, 2019, doi: 10.22266/IJIES2019.0228.22.

[42]. J. Ramkumar and R. Vadivel, "CSIP—cuckoo search inspired protocol for routing in cognitive radio ad hoc networks," in *Advances in Intelligent Systems and Computing*, 2017, vol. 556, pp. 145–153. doi: 10.1007/978-981-10-3874-7_14.

[43]. J. Ramkumar, C. Kumuthini, B. Narasimhan, and S. Boopalan, "Energy Consumption Minimization in Cognitive Radio Mobile Ad-Hoc Networks using Enriched Ad-hoc

On-demand Distance Vector Protocol," *2022 Int. Conf. Adv. Comput. Technol. Appl. ICACTA 2022*, pp. 1–6, Mar. 2022, doi: 10.1109/ICACTA54488.2022.9752899.

[44]. J. Ramkumar and R. Vadivel, "Whale optimization routing protocol for minimizing energy consumption in cognitive radio wireless sensor network," *Int. J. Comput. Networks Appl.*, vol. 8, no. 4, pp. 455–464, 2021, doi: 10.22247/ijcna/2021/209711.

[45]. J. Ramkumar and R. Vadivel, "Meticulous Elephant Herding Optimization based Protocol for Detecting Intrusions in Cognitive Radio Ad Hoc Networks," *Int. J. Emerg. Trends Eng. Res.*, vol. 8, no. 8, pp. 4548–4554, 2020, doi: 10.30534/ijeter/2020/82882020.

[46]. X. Bi *et al.*, "The Genetic-Evolutionary Random Support Vector Machine Cluster Analysis in Autism Spectrum Disorder," *IEEE Access*, vol. 7, pp. 30527–30535, 2019, doi: 10.1109/ACCESS.2019.2902889.

[47]. N. Chaitra, P. A. Vijaya, and G. Deshpande, "Diagnostic prediction of autism spectrum disorder using complex network measures in a machine learning framework," *Biomed. Signal Process. Control*, vol. 62, p. 102099, 2020, doi: https://doi.org/10.1016/j.bspc.2020.102099.